

**Big Data Supplement: Advances in spatio-temporal models
for non-communicable disease surveillance**

Journal:	<i>International Journal of Epidemiology</i>
Manuscript ID	IJE-2018-09-1139.R2
Manuscript Type:	Supplement [approved only]
Date Submitted by the Author:	07-May-2019
Complete List of Authors:	Blangiardo, Marta; Imperial College London, Department of Epidemiology and Biostatistics, School of Medicine Boulieri, Areti; Imperial College London, Department of Epidemiology and Biostatistics, School of Medicine Diggle, P; Lancaster University Faculty of Health and Medicine, Medical School Piel, Frédéric; Imperial College London, Epidemiology & Biostatistics Shaddick, G; Exeter University, Mathematics Elliott, Paul; Imperial College Londofn, Department of Epidemiology & Biostatistics
Key Words:	surveillance, non-communicable diseases, Bayesian hierarchical models, spatio-temporal modelling

1 **Advances in spatio-temporal models for non-communicable** 2 **disease surveillance**

3 Blangiardo, M.^{1,2}, Boulieri, A.², Diggle, P.³, Piel, F.B.^{1,2}, Shaddick, G.⁴ & Elliott, P.^{1,2}

4
5 ¹ *UK Small Area Health Statistics Unit, Department of Epidemiology & Biostatistics, School*
6 *of Public Health, Imperial College London, London, UK*

7 ² *MRC-PHE Centre for Environment & Health, Department of Epidemiology & Biostatistics,*
8 *School of Public Health, Imperial College London, London, UK*

9 ³ *Centre for Health Informatics, Computing and Statistics (CHICAS), Lancaster Medical*
10 *School, Lancaster University, Lancaster, UK*

11 ⁴ *Department of Mathematics, University of Exeter, Exeter, UK*

12 13 **Abstract**

14 Surveillance systems are commonly used to provide early warning detection or to
15 assess an impact of an intervention/policy. Traditionally, the methodological and
16 conceptual frameworks for surveillance have been designed for infectious diseases,
17 but the rising burden of non-communicable diseases (NCDs) worldwide suggests a
18 pressing need for surveillance strategies to detect unusual patterns in the data and to
19 help unveil important risk factors in this setting. Surveillance methods need to be able
20 to detect meaningful departures from expectation and exploit dependencies within
21 such data to produce unbiased estimates of risk as well as future forecasts. This has
22 led to the increasing development of a range of space-time methods specifically
23 designed for NCD surveillance.

24 We present an overview of recent advances in spatio-temporal disease surveillance
25 for NCDs using hierarchically specified models. This provides a coherent framework
26 for modelling complex data structures, dealing with data sparsity, exploiting
27 dependencies between data sources and propagating the inherent uncertainties
28 present in both the data and the modelling process. We then focus on three commonly
29 used models within the Bayesian Hierarchical Model (BHM) framework and through a
30 simulation study we compare their performance.

1
2
3 31 We also discuss some challenges faced by researchers when dealing with NCD
4
5 32 surveillance, including how to account for false detection and the modifiable areal unit
6
7 33 problem. Finally, we consider how to use and interpret the complex models, how
8
9 34 model selection may vary depending on the intended user group and how best to
10
11 35 communicate results to stakeholders and the general public.

12
13 36 **Keywords:** surveillance, non-communicable diseases, Bayesian hierarchical models,
14
15 37 spatio-temporal modelling.
16
17
18

19 38

20 21 39 **Key messages**

- 22
23
24 40 - There is increasing recognition of the importance of surveillance for NCDs.
25
26 41 - Spatio-temporal variation in health outcomes and lifestyle and environmental
27
28 42 exposures needs to be explicitly modelled in order to reduce bias and
29
30 43 uncertainty.
31
32 44 - Hierarchical modelling provides a coherent framework within which spatio-
33
34 45 temporal dependencies can be explicitly modelled with integration of the
35
36 46 uncertainties associated both with the data and the modelling process.
37
38 47 - In a simulation study, we found that mixture models designed for detection
39
40 48 perform better than standard disease mapping models. However, attention
41
42 49 should be paid to the choice of threshold as this impacts the results. It is
43
44 50 recommended that a simulation study based on the characteristics of the data
45
46 51 in hand is run each time for the selection of suitable threshold values.
47
48 52 - Current research challenges in this area include: the use of data from multiple
49
50 53 sources at different spatial and temporal scales and with different sources of
51
52 54 bias and uncertainty; computationally intense processes; and control for false
53
54 55 positive findings.
55
56
57
58
59
60

56

57 **1. The importance of non-communicable diseases**

58 According to the World Health Organization surveillance is the “ongoing systematic
59 data collection, analysis, interpretation and dissemination of information in order for
60 action to be taken” [1]. National public health agencies, such as the US Centers for
61 Disease Control and Prevention (CDC) and Public Health England (PHE) routinely
62 carry out surveillance data analysis to provide early warnings of unexplained changes
63 in incidence patterns of diseases as well as to aid policy formation and resource
64 allocation [2]. Specific examples include the international influenza monitoring system
65 which started in 1948 and is now distributed in 82 countries [3], the HIV and AIDS
66 Reporting System (HARS) used by PHE [4] and the National HIV Surveillance System
67 used by CDC [4].

68 To date, the majority of methods and models commonly used in public health
69 surveillance are designed for monitoring cases of infectious diseases [6]. Due to the
70 rising burden of non-communicable diseases (NCDs) worldwide, there is a pressing
71 need to implement surveillance strategies to detect trends, highlight unusual changes
72 and consequently assist in outlining emerging NCD risk factors. NCD surveillance
73 shares many objectives with infectious disease surveillance, including generating
74 information to guide public health action, detecting the health impact of environmental
75 exposures, or of environmentally driven disease vectors; however, it also presents
76 some different methodological challenges [7, 8].

77 Health data contain both a time and a space component. Surveillance methods must
78 be able to capture spatial and temporal patterns in both lifestyle/environmental
79 exposures and health outcomes. Here, we present an overview of the approaches
80 developed for spatio-temporal disease surveillance of NCDs. We focus on model-

1
2
3 81 based methods and among these on Bayesian hierarchical models (BHMs), which can
4
5 82 naturally accommodate complex data structures, as well as propagate uncertainty due
6
7 83 to the data themselves and the modelling process.
8
9

10 84 In this Section, we first discuss how data availability is one of the key challenges in
11
12 85 surveillance studies, before giving a generic overview of test-based approaches for
13
14 86 NCD surveillance. We then focus on BHMs (Section 2) and describe disease mapping
15
16 87 and mixture-based models for anomaly detection. In Section 3, we introduce the
17
18 88 computational aspects of the BHM modelling framework for NCD surveillance, while
19
20 89 in Section 4 we run a simulation study to evaluate advantages and drawbacks of the
21
22 90 approaches presented in detecting areas deviating from the expected trend. Finally,
23
24 91 in Section 5 we conclude with a summary and some remaining discussion points.
25
26
27
28
29

30
31
32 92

33 93 1.1 Data availability

34 94 One of the major challenges of surveillance studies is the availability of suitable data.
35
36 95 This applies to both infectious disease and NCD surveillance. It is a particularly
37
38 96 important issue in low-income settings because surveillance studies often need to rely
39
40 97 on information from surveys, and the lack of financial resources may make
41
42 98 comprehensive coverage of data sources (e.g. mortality/cancer registries) over an
43
44 99 entire country infeasible [9].
45
46

47 100 In the last 15 years, a number of Health and Demographic Surveillance Systems
48
49 101 (HDSS) have been established in low-income settings to provide a reliable source of
50
51 102 health data and are now linked together through the International Network for the
52
53 103 Continuous Demographic Evaluation of Populations and Their Health (INDEPTH, [10]).
54
55 104 Such continuous surveys are an invaluable source of data, but researchers face issues
56
57 105 related to population representativeness. A recent study proposed a Bayesian
58
59
60

1
2
3 106 probabilistic clustering method to evaluate the network representativeness in terms of
4
5 107 socio-economic and environmental variables in sub-Saharan Africa, identifying areas
6
7 108 of poor coverage in the existing network and using predictive probability distributions
8
9 109 to suggest the best location for new HDSS sites [11].
10
11

12 110 Even in high income settings where administrative resources are available for the
13
14 111 entire population, there may be issues regarding the population at risk, used as
15
16 112 denominator in the risk estimates. In small-area studies on mortality or hospital
17
18 113 admissions, the denominator is usually the resident population in each administrative
19
20 114 area, typically estimated from national census statistics, but there may be estimation
21
22 115 problems for inter-censal years. In addition, it is not straightforward to define the
23
24 116 denominator where the interest is for less-defined geographies, such as the catchment
25
26 117 areas of clinical centres (e.g. general practices in England).
27
28
29

30 118 Furthermore, the availability of administrative or health data may become more limited:
31
32 119 for instance, within the UK National Health Service, patients can now decide not to
33
34 120 share their medical records for research purposes. This clearly impacts on spatial
35
36 121 coverage and could potentially lead to biased statistical inference if the data gaps are
37
38 122 clustered in space and/or if they differentially affect specific population groups (e.g.
39
40 123 elderly, more deprived) [12].
41
42
43

44 124

45 46 47 125 1.2 Test-based methods

48
49 126 Methods for NCD surveillance have largely been based around the idea of detecting
50
51 127 whether the outcome of interest shows a particular behaviour in a defined subset (e.g.
52
53 128 an area, period of time, or combination of space and time) when compared to the
54
55 129 whole study region. Perhaps the most popular test-based methods used for NCD
56
57 130 surveillance are the scan statistics. These were developed originally in the temporal
58
59
60

1
2
3 131 setting only [13]; here, a fixed length “scanning window” is passed over the time-series
4
5 132 data with the number of cases in the window being recorded. A log likelihood ratio
6
7 133 (LLR) is calculated for each interval, and the test statistic is defined as the maximum
8
9 134 LLR over all intervals. This idea was extended to a spatial version of the scan statistic
10
11 135 [23, 15], which was later further extended to the spatio-temporal setting [16]. In this
12
13 136 case, the scanning window is represented by a cylinder, where the diameter specifies
14
15 137 the spatial dimension and the height the temporal dimension. An additional version of
16
17 138 spatial scan statistic was proposed to account for correlation across spatial units which
18
19 139 was not considered before [17]. Scan statistics have been extensively applied to
20
21 140 numerous health care applications. Part of their popularity lies in the availability of free
22
23 141 user-friendly SaTScan™ software (<https://www.satscan.org/>). Recent applications of
24
25 142 SaTScan include the identification of signals for colorectal cancer [18], drug activity
26
27 143 [19], criminality [20], and bat activity [21].
28
29 144 A further development has been the detection of spatial variations in temporal trends
30
31 145 (SVTT). These methods extend the scan statistics to estimate the time trend via a
32
33 146 regression-based model specifying either a linear or a quadratic function. The
34
35 147 quadratic SVTT method has, for example, been applied to cervical cancer data in
36
37 148 women in the US from 1969 to 1995 highlighting areas where the risk was significantly
38
39 149 different from the rest [22].
40
41 150 Test-based methods such as scan statistics can only answer questions related to the
42
43 151 deviation from the null hypothesis. An alternative approach is to explicitly model the
44
45 152 spatio-temporal structure in the data and to assess whether differences between
46
47 153 observed data and those predicted from the model provide evidence of anomalies.
48
49 154 There are a number of advantages to adopting a model-based approach over a test-
50
51 155 based method including the ability to: (i) have more statistical power to handle sparsity
52
53
54
55
56
57
58
59
60

1
2
3 156 in the observed disease counts; (ii) explore more subtle departures from the
4
5 157 expectation; (iii) account for the spatial and temporal correlation that is typically evident
6
7 158 in health data; (iv) “borrow” information over space and time, therefore increasing the
8
9 159 precision of the estimates generated; (v) include covariates that might explain some
10
11 160 of the spatio-temporal variability.
12
13
14
15

161 **2. Hierarchical models and likelihood-based inference**

162 Hierarchical models (HM) are able to deal with complex data structures, to exploit
163 dependencies between data sources and to propagate the inherent uncertainties that
164 are present in both the data and the modelling process. In the current context, an HM
165 combines two elements: a *process model* that describes how disease risk varies over
166 space and time, typically involving both extant covariate effects and a latent spatio-
167 temporal stochastic process; and a *data model* that describes the statistical properties
168 of the available health outcome data conditional on the realisation of the underlying
169 risk process. Both elements are specified up to the values of a set of unknown
170 *parameters*, which can be estimated by Bayesian or non-Bayesian versions of
171 likelihood-based inference, typically implemented using Markov chain Monte Carlo
172 integration and Monte Carlo likelihood maximisation methods, respectively. In addition
173 to estimating parameters, the scientific goals of health surveillance include *prediction*
174 of relevant properties of the unobserved risk surface as it evolves in real-time.
175 Parameters and latent stochastic processes are fundamentally different things, but
176 within the Bayesian paradigm they are both treated as unobserved sets of random
177 variables, and the operational calculus of estimation and prediction coalesces. In what
178 follows, we use BHM (Bayesian Hierarchical Modelling) as a shorthand for Bayesian
179 inference applied to a hierarchically specified model.

180

181 2.1 Space-time disease mapping

182 A class of BHMs that has been extensively used for the analysis of NCD data are the
183 so-called disease mapping models (DM). These are hierarchical models in which the
184 latent component of area-level disease risk is modelled as a spatially discrete Markov
185 random field [23] and, depending on the sampling design, the conditional distribution
186 of area-level case-counts is Poisson or Binomial [24, 25, 26, 27]. While the objectives
187 of these are descriptive, they have been used as the basis for the development of
188 detection models, which are framed in a surveillance perspective. Disease mapping
189 models have been extensively used to estimate and visualise the spatial or spatio-
190 temporal distribution of a disease (see for instance [9, 21, 28]).

191 Spatial dependence in the latent component of a DM is modelled by specifying
192 neighbourhood relationships amongst the area-level risks, the most widely used
193 definition being that two areas are *neighbours* if they share a common boundary. A
194 common choice for capturing temporal dependence is a random walk prior [29], but
195 extensions to incorporate spatio-temporal interactions among neighbouring areas and
196 time points have also been developed [30]. This framework can also account for
197 factors known to modify spatial and temporal trends that, in the context of NCDs, will
198 include demographic variables (e.g. age/sex/ethnicity) and social economic status.
199 Random effects can be assigned for each factor (with appropriate priors) and for
200 interactions if required. An example is provided by Goicoa *et al.* [31] who proposed a
201 space-time-age model to study prostate cancer incidence across 50 provinces in
202 Spain for 9 age groups over 25 years, accounting for all pair-wise interactions. The
203 authors used ranking of all provinces according to mortality rates to identify high-risk
204 groups.

1
2
3 205 A key characteristic of BHMs is the ready availability of joint posterior/predictive
4
5 206 distributions for parameters/latent processes and whatever of their properties are
6
7 207 relevant to the public health questions of interest. In the context of disease mapping
8
9 208 this leads to a spatial, temporal and spatio-temporal risk distribution that researchers
10
11 209 can map, both in terms of point estimates but also of associated measures of
12
13 210 uncertainty. For the latter, a common choice is the predictive probability that the
14
15 211 relative risk exceeds a pre-specified threshold [32, 33]. Exceedance probabilities can
16
17 212 be used to flag areas and/or time points characterised by increased risk that may then
18
19 213 be further investigated. In this way, disease mapping, though not formally a
20
21 214 surveillance method, can be used as a descriptive tool for the identification of areas
22
23 215 and/or time periods with marked deviation from expectation. It is important to note that
24
25 216 the strong smoothing effect of disease mapping models leads to conservative risk
26
27 217 estimates, hence to a small number of false positive findings, at the expense of a low
28
29 218 power for detecting high risk areas with low signal. To minimise that, an extensive
30
31 219 simulation was run to find the best threshold on the exceedance probability scale to
32
33 220 classify an area as high risk [33]. The authors showed that a good trade-off between
34
35 221 false-positive and false-negative rates is achieved with a probability above 0.8 for a
36
37 222 relative risk to be higher than 1, however this largely depends on the number of
38
39 223 expected counts, the number of areas and time points, and the spatial risk [34].
40
41 224 As an example of the typical disease mapping output, Figure 1 shows the incidence
42
43 225 of malignant melanoma in males, at the census ward level in England and Wales over
44
45 226 the period 1985-2009 from the Environmental and Health Atlas produced by the UK
46
47 227 Small Area Health Statistics Unit (SAHSU) [35]; the map on the left presents the spatial
48
49 228 distribution of the posterior relative risk mean estimates, while the map on the right
50
51
52
53
54
55
56
57
58
59
60

1
2
3 229 plots the posterior probability that the corresponding relative risk is above 1, using the
4
5 230 categorisation suggested in [33].
6

7
8 231  Figure 1 here
9

10 232 Disease mapping models can be extended to two or more outcomes that might share
11
12 233 spatial (and temporal) patterns, for instance due to common risk factors. A joint model
13
14 234 allows information to be borrowed across the outcomes, thus helping stabilise
15
16 235 estimates, particularly when the outcomes are rare. The shared component model [36],
17
18 236 originally developed for two diseases, includes a common component (likely to reflect
19
20 237 common risk factors), and a disease-specific one, which can point towards specific
21
22 238 risk factors otherwise masked in a single disease model. It was applied to male and
23
24 239 female lung cancer [37] and later extended to jointly model multiple diseases [30, 38],
25
26 240 with an application on oral cavity, oesophagus, larynx and lung cancers in males in
27
28 241 the 544 districts of Germany from 1986 to 1990. Recently, it was further extended to
29
30 242 jointly model age- and gender-specific diseases [39].
31
32

33
34 243 An alternative multivariate specification considers spatial and temporal terms explicitly,
35
36 244 modelling the correlation among the outcomes in space/time. As an example, road
37
38 245 traffic accidents characterised by different severity were analysed over the period
39
40 246 2005-2011 at the ward level in England while detection of high-risk areas was
41
42 247 performed using exceedance probabilities of the area ranks based on accident rates
43
44 248 [40].
45
46

47
48
49 249

50 250 2.2 Space-time anomaly detection

51
52 251 The standard disease mapping approach has been used informally to detect
53
54 252 anomalies (unusual observations) in space and time, i.e. areas and/or time points with
55
56 253 trends different to the expected ones, adding a space-time interaction parameter into
57
58
59
60

1
2
3 254 the latent process [37]. The detection of anomalies may indicate the presence of an
4
5 255 emerged localised risk factor, the impact of an intervention, or differences in the quality
6
7
8 256 of data, such as misdiagnosis of a disease, and under- or over-reporting of cases.
9

10 257 Mixture models have been proposed as a formal approach to anomaly detection. In
11
12 258 particular, Abellan *et al.* [41], developed a BHM model (termed STmix) where a mixture
13
14 259 of two normal distributions characterised by different variances is specified for the
15
16 260 space-time interaction. Then, the interaction is used to classify areas as *common* and
17
18 261 *unusual*. The authors performed a simulation study to compare the method against
19
20 262 the standard disease mapping approach. The results of the simulation study showed
21
22 263 that the standard approach was not able to capture the variability in the spatio-
23
24 264 temporal interactions and therefore it was not able to distinguish between common
25
26 265 and unusual areas. This is due to the excessive smoothing following the assumption
27
28 266 of a common variance across all the areas and time points. STmix was applied to
29
30 267 mammography screening data in Brisbane, Australia, at the statistical local area (SLA)
31
32 268 level, from 1997 to 2008 in order to identify SLAs whose temporal trend exhibited
33
34 269 volatility [42]. A well-known drawback of this approach is its limitation to incorporate
35
36 270 specific time patterns, for example step changes that could signal the emergence of a
37
38 271 new risk factor.
39
40
41
42
43

44 272 Another mixture model, proposed by Li *et al.* [43], accommodates this issue. Here, the
45
46 273 mixture specification of the method is defined directly on the relative risks in space
47
48 274 and time, to allow for detection of areas with unusual time trends rather than space-
49
50 275 time deviations. In particular, two alternative models are considered: the first one
51
52 276 assumes a global time trend for all areas (*common trend*), while the second estimates
53
54 277 a time trend for each area independently (*area-specific trend*). Through a simulation
55
56 278 study the authors showed better performance in terms of both sensitivity and
57
58
59
60

1
2
3 279 proportion of false positives compared to SaTScan on a wide range of scenarios. This
4
5 280 approach, named BaySTDetect, was applied to detect unusual trends for asthma and
6
7 281 chronic obstructive pulmonary disease at Clinical Commissioning Group (CCG) level
8
9 282 in England (211 in total) on monthly data between August 2010 and March 2011
10
11 283 across mortality, hospital admissions, and general practice drug prescriptions [44].
12
13 284 To illustrate the typical output obtained from this model, Figure 2 shows the area-
14
15 285 specific time trends of the CCGs that were detected as unusual plotted against the
16
17 286 national trend. Other applications of this method include burglary data [45], gray whale
18
19 287 abundance [46] and mammography data [42].
20
21
22
23

24 288 Figure 2 here

25
26 289 This method was further extended to increase its flexibility by accounting for different
27
28 290 space-time patterns in the unusual observations, as well as by allowing for longer time
29
30 291 series to be analysed. This improved method, termed FlexDetect, had a better
31
32 292 performance when compared to the original method through an extensive simulation
33
34 293 study [47].
35
36

37 294 *Multiple testing*

38
39 295 As surveillance studies involve evaluating trends for different health outcomes, many
40
41 296 areas and different time periods at the same time, false detections are likely to occur
42
43 297 by chance. Bonferroni correction has been extensively used in epidemiology to correct
44
45 298 for multiple testing, particularly in omics studies [48, 49], but it is well known that this
46
47 299 approach leads to conservative results. Benjamini and Hochberg first introduced an
48
49 300 alternative index, the false discovery rate (FDR) [50], as the expected value of the rate
50
51 301 of false positive findings among all rejected hypotheses and used it in a frequentist
52
53 302 approach. The same method was suggested in the context of descriptive spatial
54
55 303 epidemiology, to obtain areas characterised by a Standardised Mortality Ratio different
56
57
58
59
60

1
2
3 304 from 1 [51]. Even in the Bayesian setting, FDR rules were suggested by many authors
4
5 305 [52, 53, 54, 55, 56]. The mixture model proposed by Li et al. uses the specification
6
7 306 suggested by Newton et al. [53] later used by Ventrucchi et al. [57] in order to account
8
9 307 for multiple testing. The authors base the FDR statistic on the posterior model
10
11 308 probability, which represents the likelihood of the space-time unit investigated to follow
12
13 309 the common trend model, i.e. to exhibit a risk pattern not deviating from the expected
14
15 310 one [43].

16
17
18
19 311 While the importance of controlling for multiple testing is clear in classical significance
20
21 312 testing, the analogous problem in predictive setting is less of a concern [58]. One
22
23 313 reason for this is that local predictions from hierarchical models are naturally smoothed
24
25 314 towards the global mean, making these consequently less prone to false positive
26
27 315 findings than unsmoothed area-by-area interval estimates. Another is that the Monte
28
29 316 Carlo sampling method allows the computation of whatever joint probability statements
30
31 317 are required. For example, if the public health question is whether current risk exceeds
32
33 318 an agreed acceptable level in all areas that do, and in no areas that do not, meet a
34
35 319 particular criterion such as adherence to a particular advisory policy, the correct
36
37 320 predictive probability to attach to this statement can be calculated.

321 **3. Computational aspects**

322 One of the biggest challenges researchers face when analysing large and complex
323 space-time datasets is their computational burden. This applies particularly in the
324 small-area context, where the number of space-time units investigated can vary
325 substantially depending on the chosen spatial and temporal resolution, from few
326 hundreds to hundreds of thousand units, particularly when several outcomes are jointly
327 analysed (for instance Foreman et al. [59] considered jointly deaths/age/sex specific
328 space-time trends in the U.S).

1
2
3 329 The degree of complexity of the model (e.g. the number of parameters) also impacts
4
5 330 on the computational burden, for instance in terms of convergence time when running
6
7 331 MCMC simulations. Under the Bayesian paradigm, the choice of the prior will also
8
9 332 influence convergence; an informative prior, assuming that there is no conflict with the
10
11 333 data, will normally speed up convergence, while a vague prior will most likely lead to
12
13 334 longer time to reach convergence. Finally, the choice of software used for the analysis
14
15 335 will affect the model running time. The user-friendly software BUGS (Bayesian
16
17 336 inference Using Gibbs Sampling) [60] has been traditionally used for Bayesian
18
19 337 inference using MCMC methods, however it can be slow when high dimensional data
20
21 338 and/or complex models are used. Other MCMC-based methods, such as Stan [61]
22
23 339 and NIMBLE [62], are currently attracting attention due to their active development
24
25 340 community. An alternative way of dealing with computational limitations is to use
26
27 341 approximative methods; for instance INLA (integrated nested Laplace approximations)
28
29 342 [63] has been successfully used for running space-time disease mapping models (e.g.
30
31 343 [31, 64]); however, this method is somewhat less flexible than the aforementioned
32
33 344 ones and as it relies on Normality of the latent process is not able to deal with mixture
34
35 345 distributions.
36
37 346 Computationally intensive BHMs benefit from high-performance computing clusters to
38
39 347 speed up computation times, however these are not necessarily required. For instance
40
41 348 in [40] road traffic accidents data of different severity in England were analysed
42
43 349 simultaneously at the ward level (~8000), over 9 years (for a total of around 150,000
44
45 350 units and 32,000 parameters); the analysis was run in OpenBUGS and took 20 to 27hr
46
47 351 on an Intel Core processor at 3.40 GHz with 8 Gbytes of random-access memory. On
48
49 352 a much bigger scale, a US small area study considered more than half a million units
50
51
52
53
54
55
56
57
58
59
60

1
2
3 353 and nearly 6,000 parameters [59]; the analysis was implemented in Stan using higher
4
5 354 performance computing (HPC) clusters for faster calculations.
6
7
8

9 355 **4. Simulation-based example**

10
11 356 Considering the multitude of space-time methods available, as described above, it is
12
13 357 important to formally evaluate their respective detection performance. In this paper we
14
15 358 carried out a simulation study to formally evaluate the detection performance and
16
17 359 compare DM, STmix and FlexDetect (see description of the models in Section 2.2).
18
19 360 Following the design initially proposed by [43], and later used by [47], we used real
20
21 361 asthma hospital episode statistics (HES) data to generate 50 simulated datasets. The
22
23 362 asthma dataset was obtained from SAHSU, Imperial College London and consisted of
24
25 363 disease counts across 211 Clinical Commissioning Groups (CCG) in England for 15
26
27 364 months, from January 2010 to March 2011. The 50 simulated datasets were generated
28
29 365 to closely resemble the patterns seen in the real dataset. A standard spatio-temporal
30
31 366 model [27] was first fitted to the real data and the obtained parameters were selected
32
33 367 for the generation of the simulated data. We selected 15 areas to deviate from the
34
35 368 overall time trend over the last 5 time points. For these 15 areas, we selected the
36
37 369 signal to be increased by $\log(2)$ for time points 3 and 10, and decreased by $\log(2)$ for
38
39 370 time points 6, 12 and 15 out of the total 15 time points. In this way, we ensured that a
40
41 371 realistic scenario was used (for more details see [47] Supplementary materials,
42
43 372 Scenario 1). The R code used for the data simulation, together with the three models
44
45 373 written in BUGS can be found on <https://github.com/aretib/bayesSTmodels.git>.
46
47 374 The results are presented in Table 1 in terms of four different performance measures.
48
49 375 We defined TP as the number of true positives, FP as false positives, TN as true
50
51 376 negatives and FN as false negatives respectively. Sensitivity measures the ability of
52
53 377 the model to correctly classify an unusual observation as such, defined as $TP/(TP+FN)$,
54
55
56
57
58
59
60

1
2
3 378 and similarly specificity measures the ability of the model to correctly classify a
4
5 379 common observation as such ($TN/(TN+FP)$). In addition, it is crucial to control the
6
7 380 proportions of observations that are falsely classified as unusual (false discovery rate
8
9 381 (FDR)) and common (false omission rate (FOR)) respectively; these should typically
10
11 382 not exceed a value of 0.05, specified based on the standard p-value threshold. We
12
13 383 consider (i) two different thresholds for DM: 0.8 as commonly used and previously
14
15 384 described (DM1); a more conservative threshold of 0.9 (DM2), under the assumption
16
17 385 that false positives are more important to minimise than false negatives, and (ii) two
18
19 386 different rules for STmix as presented in the original paper: an area is modified if at
20
21 387 least for one time point the space-time interaction has a probability greater than 0.8 to
22
23 388 be above 1 (STmix1); an area is modified if for at least three time points the space-
24
25 389 time interactions have an average probability greater than 0.8 to be above 1 (STmix2).
26
27
28
29

30
31 Table 1 here
32

33 391 As can be seen, the disease mapping approach using the standard threshold of 0.8
34
35 392 on the posterior probability scale (DM1) shows the worst performance; as expected
36
37 393 the method is able to detect nearly all unusual areas, with a sensitivity of 0.979;
38
39 394 however, roughly 79% of the detected findings are not actually unusual (FDR = 0.785)
40
41 395 (Table 1). Fixing a 0.9 threshold (DM2), FDR decreases, despite still being above the
42
43 396 standard threshold of 0.05, while at the same time sensitivity also decreases (0.660)
44
45 397 (Table 1).
46
47
48

49 398 The two mixture models returned more comparable performances. STmix1 gave no
50
51 399 false positive results (FDR = 0) and a sensitivity of 0.773, while for STmix2 sensitivity
52
53 400 increased to 0.969, but at the same time a much higher proportion of false positive
54
55 401 was detected (FDR = 0.220). The results of FlexDetect provided a balance between
56
57
58
59
60

1
2
3 402 the two extremes, giving a proportion of FDR equal to 0.019 and a sensitivity of 0.796.
4
5 403 In terms of specificity and FOR, both STmix and FlexDetect behave similarly.
6
7 404 Differences across the competing models were observed in terms of computation time,
8
9 405 an important factor in assessing their performance. All models were run in an Intel
10
11 406 Xeon Core processor 3.40GHz with 125GB RAM. Each of the 50 simulations took on
12
13 407 average 33.4 mins for models DM1 and DM2, 39.2 mins for models STmix 1 and
14
15 408 STmix2 and 66.8 mins for FlexDetect. The simulation results suggest that using
16
17 409 disease mapping (DM) for surveillance purposes is not appropriate and that one of the
18
19 410 mixture models designed for detection should be used instead. Between STmix and
20
21 411 FlexDetect it is worth mentioning that STmix can only identify areas where anomalies
22
23 412 are present, and not the time points when these occur. In addition to this, its detection
24
25 413 mechanism does not consider specific patterns in the time trends. These can be
26
27 414 accommodated by FlexDetect, which however is more computationally intensive. Also
28
29 415 note that mixture models notoriously have problems converging, suffering from issues
30
31 416 such as label switching, which lead to multimodal posterior distributions. Both the
32
33 417 detection methods deal with this through the modelling specification, such as [41]
34
35 418 constraining the variance of the modified areas to be larger than that of unmodified
36
37 419 areas, or through informative priors on the variances of the two components [43].
38
39
40
41
42
43
44
45

420 **5. Discussion**

421 In this paper we have presented an overview of the main statistical methods for
422 disease surveillance in the context of NCDs, both from a test-based and model-based
423 perspective and with a particular focus on the BHM approach, which provides a flexible
424 framework to allow for complex data dependencies present in surveillance studies.
425 Through a simulation study we showed that disease mapping is not satisfactory when
426 looking for data anomalies, while the two methods based on mixture models provide

1
2
3 427 a better compromise between detecting areas characterised by a deviation from the
4
5 428 expected trend and limiting false positives. Note that our perspective is on methods
6
7 429 that detect single areas, rather than clusters of adjacent spatial units. If the interest
8
9 430 lays on detection in the presence of spatial proximity, recent methods have been
10
11 431 developed to combine clustering with spatial smoothing, see for example [65] and [66].
12
13 432 An interesting aspect of the general hierarchical framework presented is that it can
14
15 433 easily incorporate forecasting of the disease risk, which is relevant in the context of
16
17 434 epidemiological surveillance to evaluate the need for resources/policies/costs in
18
19 435 specific areas and future time points. Some work in this area includes Foreman et al.,
20
21 436 [59] who, using annual vital statistics for 1974-2011 at the US state spatial resolution,
22
23 437 forecasted mortality up to 2024, while Ugarte et al. [67] used P-splines to forecast
24
25 438 cancer mortality counts in Spanish regions for 2009-2011 using data from 1975-2008.
26
27 439 Most of the work presented is based on routinely collected data for retrospective
28
29 440 studies. However, there is increased importance of early warning detection, so that
30
31 441 unusual behaviour can be detected at the earliest possible time. Syndromic data, such
32
33 442 as primary care data, drug prescriptions, nurse calls and home visits, which are
34
35 443 indicative of a potential anomaly, may provide an additional level of information leading
36
37 444 to a detection event before the data aberration occurs [68]. Diggle et al. [69, 70]
38
39 445 analysed NHS non-emergency telephone calls reporting symptoms of gastrointestinal
40
41 446 diseases. The authors specified a spatio-temporal point process on the location and
42
43 447 time of the individual calls and modelled the spatial and temporal dependency on the
44
45 448 intensity of the process. They used exceedance probabilities to define maps of
46
47 449 potential outbreaks. Another example can be found in Morrison et al. [71]
48
49 450 who forecasted multiple measures of healthcare utilization (including physician visits
50
51 451 and prescriptions of asthma medication) within British Columbia, Canada, where
52
53
54
55
56
57
58
59
60

1
2
3 452 seasonal wildfires produce high levels of air pollution, significantly impacting
4
5 453 population health. Here, the focus was on efficient, near real-time, computation which
6
7 454 was achieved using INLA to perform approximate Bayesian inference.
8
9

10 455 Potentially syndromic information can also be linked with routine data such as Hospital
11
12 456 Episode Statistics and provide predictors in order to obtain a better description of the
13
14 457 data and more accurate one-step-ahead forecasts. Lately work has been done to take
15
16 458 advantage of the rich data from social media in a surveillance perspective. For
17
18 459 instance, Dai et al. [72] linked tweets with the American Community Survey and the
19
20 460 Behavioral Risk Factor Surveillance System to study asthma prevalence at the State
21
22 461 level in the US. The authors claimed that the inclusion of social media data could be
23
24 462 a cost-effective real time health detection system. However, there may be challenges
25
26 463 in future due to selective data availability following perceived concerns about data
27
28 464 security and confidentiality, as demonstrated by the newly implemented NHS National
29
30 465 Data Optout Programme. This will potentially lead to bias in population
31
32 466 representativeness due to non-random missingness [12] which will need to be
33
34 467 addressed using advanced statistical methods, for instance through the integration of
35
36 468 data from appropriate surveys / cohorts, as proposed in the context of residual
37
38 469 confounding [73].
39
40
41
42
43

44 470 An important issue with surveillance studies is that of the spatial resolution and the
45
46 471 type of geographical areas considered; modifying these might lead to different results,
47
48 472 as the spatial distribution of the outcome will depend on these choices. For instance,
49
50 473 if within-area variability is substantial, results from statistical inference might suffer
51
52 474 from false negative observations, as potentially high-risk places are aggregated with
53
54 475 low-risk ones. The more spatial variability is present in the data, the more profound
55
56 476 the potential impact of the modifiable areal unit (MAUP) [74, 75]. As MAUP depends
57
58
59
60

1
2
3 477 on the level of aggregation, this issue has been linked to ecological bias [76] and the
4
5 478 general suggestion in the scientific literature is to consider the finest spatial scale
6
7 479 available. This can be particularly challenging for rare diseases where the number of
8
9 480 cases at small-area level are very low. Furthermore, the choice of spatial resolution is
10
11 481 mostly dependent on data availability and sparsity. BHMs have been suggested as a
12
13 482 way to, at least partially, deal with MAUP. As there is an explicit relationship among
14
15 483 areas globally and/or locally, through structured random effects, places belonging to
16
17 484 a particularly small area can influence results for other areas, hence alleviating the
18
19 485 MAUP problem [77].
20
21
22

23 486 A key aspect of surveillance studies concerns how to communicate information to
24
25 487 public health researchers and policy makers. This is particularly challenging as the
26
27 488 statistical modelling of surveillance data becomes more sophisticated. In this context
28
29 489 it is essential to develop user friendly tools such as atlases, web applications and
30
31 490 reporting services that allow for data visualisations and easy implementation of the
32
33 491 advanced methodologies. The Environment and Health Atlas for England and Wales
34
35 492 [35] (typical output from the Atlas was presented in Figure 1) is an example of work in
36
37 493 this direction, providing stakeholders and the general public with a collection of maps
38
39 494 to inform on the spatial distribution of environmental factors and diseases. Through
40
41 495 the exceedance probabilities, these maps give a perception of the uncertainty around
42
43 496 the area level relative risks estimates.
44
45
46
47

48
49 497 Web applications allow the ready implementation of statistical methods and perform
50
51 498 complex data analyses, often through interactive data visualisations. These can be
52
53 499 particularly useful for practitioners less skilful in statistical modelling and programming.
54
55 500 As an example, the Rapid Inquiry Facility (RIF) which is currently being redeveloped
56
57 501 within SAHSU, is designed to facilitate disease mapping and risk analysis studies and
58
59
60

1
2
3 502 has been employed by more than 45 institutions in a number of countries [78]. A more
4
5 503 recent example is the SpatialEpiApp that integrates two methods for disease mapping
6
7
8 504 and cluster detection [79].
9

10 505 To conclude, in this paper we presented a range of BHMs, which have proved to be
11
12 506 useful for non-communicable disease surveillance. The choice of model should
13
14 507 depend on various factors and most importantly on the objective of the study,
15
16 508 characteristics of the data, and computational resources. It is commonly
17
18 509 recommended to perform simulation studies based on the data in hand, to inform the
19
20 510 model and to select detection rules that are most appropriate in each case.
21
22

23
24 511 We believe that epidemiological surveillance will be at the centre of future
25
26 512 methodological research to match the continuous increase in data availability, e.g.
27
28 513 through social media; this will also open up issues related to data integration, selection
29
30 514 bias and spatio-temporal misalignment. At the same time there will be the need to
31
32 515 reduce the computational burden of increasingly complex models applied to large
33
34 516 datasets, in order to provide timely results for decision making.
35
36

37
38 517

39 518 **Acknowledgments**

40
41
42 519 The UK Small Area Health Statistics Unit (SAHSU) is part of the MRC-PHE Centre for
43
44 520 Environment and Health, which is supported by the Medical Research Council
45
46 521 (MR/L01341X/1) and Public Health England (PHE). Part of this work was supported
47
48 522 by an Early Career MRC Fellowship awarded to AB and a Wellcome Trust Seed Award
49
50 523 in Science awarded to FBP (204535/Z/16/Z). PE is Director of SAHSU and Director of
51
52 524 the MRC-PHE Centre for Environment and Health.
53

54
55
56 525 All authors declare no conflicts of interest.
57

58 526

59 527
60

1
2
3 528
4 529
5 530 **References**
6 531
7
8 532
9 533
10 534
11 535
12 536
13 537
14 538
15 539
16 540
17 541
18 542
19 543
20 544
21 545
22 546
23 547
24 548
25 549
26 550
27 551
28 552
29 553
30 554
31 555
32 556
33 557
34 558
35 559
36 560
37 561
38 562
39 563
40 564
41 565
42 566
43 567
44 568
45 569
46 570
47 571
48 572
49 573
50 574
51 575
52 576
53 577
54 578
55
56
57
58
59
60

1. Thacker SB, Stroup DF. Future directions for comprehensive public health surveillance and health information systems in the United States. *Am J Epidemiol* 1994; 140(5):383-97.
2. Lawson AB, Kleinman K, editors. *Spatial and syndromic surveillance for public health*. John Wiley & Sons; Chichester, England 2005.
3. World Health Organization. Global Influenza Surveillance and Response System (GISRS) [Internet]. 2018 [cited 24 April 2018]. Available from: http://www.who.int/influenza/gisrs_laboratory/en/
4. Public Health England. HIV surveillance systems [Internet]. 2008 [cited 24 April 2018]. Available from: <https://npin.cdc.gov/funding/national-hiv-surveillance-system-nhss>
5. Centers for Disease Control and Prevention. National HIV Surveillance System (NHSS) [Internet]. 2015 [cited 24 April 2018]. Available from: <https://www.gov.uk/guidance/hiv-surveillance-systems>
6. Lombardo JS, Buckeridge DL. *Disease surveillance: a public health informatics approach*. John Wiley & Sons; Chichester, England 2012.
7. Thacker SB, Stroup DF, Parrish RG, Anderson HA. Surveillance in environmental public health: issues, systems, and sources. *Am J Public Health* 1996; 86(5):633-8.
8. Frumkin H, Hess J, Lubner G, Malilay J, McGeehin M. Climate change: the public health response. *Am J Public Health* 2008; 98(3):435-45.
9. Diggle PJ, Giorgi E. Model-based geostatistics for prevalence mapping in low-resource settings. *J Am Stat Assoc* 2016; 111(515):1096-120.
10. Ye Y, Wamukoya M, Ezech A, Emina JB, Sankoh O. Health and demographic surveillance systems: a step towards full civil registration and vital statistics system in sub-Saharan Africa?. *BMC public health* 2012; 12(1):741.
11. Utazi CE, Sahu SK, Atkinson PM, Tejedor N, Tatem AJ. A probabilistic predictive Bayesian approach for determining the representativeness of health and demographic surveillance networks. *Spat Stat-Neth* 2016; 17:161-78.
12. Piel FB, Parkes BL, Daby H, Hansell AL, Elliott P. The challenge of opt-outs from NHS data: a small-area perspective. *J Public Health* 2018 (to appear).
13. Naus JL. Clustering of random points in two dimensions. *Biometrika* 1965; 52(1-2):263-6.
14. Kulldorff M, Nagarwalla N. Spatial disease clusters: detection and inference. *Stat Med* 1995; 14(8):799-810.
15. Kulldorff M. A spatial scan statistic. *Commun Stat Theory Methods* 1997; 26(6):1481-96.
16. Kulldorff M, Heffernan R, Hartman J, Assunção R, Mostashari F. A space-time permutation scan statistic for disease outbreak detection. *PLoS Med* 2005; 2(3):e59.
17. Loh JM, Zhu Z. Accounting for spatial correlation in the scan statistic. *Ann Appl Stat* 2007; 1(2):560-84.
18. Sherman RL, Henry KA, Tannenbaum SL, Feaster DJ, Kobetz E, Lee DJ. Peer Reviewed: Applying Spatial Analysis Tools in Public Health: An Example Using SaTScan to Detect Geographic Targets for Colorectal Cancer Screening Interventions. *Prev Chron Dis* 2014; 11.

1
2
3
4
5
6
7
8
9
10
11
12
13
14
15
16
17
18
19
20
21
22
23
24
25
26
27
28
29
30
31
32
33
34
35
36
37
38
39
40
41
42
43
44
45
46
47
48
49
50
51
52
53
54
55
56
57
58
59
60

- 579 19. Linton SL, Jennings JM, Latkin CA, Gomez MB, Mehta SH. Application of
580 space-time scan statistics to describe geographic and temporal clustering of
581 visible drug activity. *J Urban Health* 2014; 91(5):940-56.
- 582 20. Runadi T, Widyarningsih Y. Application of hotspot detection using spatial scan
583 statistic: Study of criminality in Indonesia. In *AIP Conference Proceedings*
584 2017 (Vol. 1827, No. 1, p. 020011). AIP Publishing.
- 585 21. Adams AM, Fenton MB. Identifying peaks in bat activity: a new application of
586 SaTScan's space-time scan statistic. *Wildl Res* 2017; 44(5):392-9.
- 587 22. Moraga P, Kulldorff M. Detection of spatial variations in temporal trends with a
588 quadratic function. *Stat Methods Med Res* 2016; 25(4):1422-37.
- 589 23. Rue H, Held L. *Gaussian Markov random fields: theory and applications*. CRC
590 press; Boca Raton, US 2005.
- 591 24. Leroux BG, Lei X, Breslow N. Estimation of disease rates in small areas: a
592 new mixed model for spatial dependence. In *Statistical models in*
593 *epidemiology, the environment, and clinical trials* (pp. 179-191). Springer,
594 New York, US 2000.
- 595 25. MacNab YC, Dean CB. Parametric bootstrap and penalized quasi-likelihood
596 inference in conditional autoregressive models. *Stat Med* 2000;
597 19(17-18):2421-35.
- 598 26. Rodrigues EC, Assunção R. Bayesian spatial models with a mixture
599 neighborhood structure. *J Multivar Anal* 2012; 109:88-102.
- 600 27. Besag J, York J, Mollié A. Bayesian image restoration, with two applications
601 in spatial statistics. *Ann Inst Stat Math* 1991; 43(1):1-20.
- 602 28. World Health Organization. *Global action plan for the prevention and control*
603 *of non communicable diseases 2013–2020*. Geneva: WHO; 2013.
604 <http://www.who.int/nmh/publications/ncd-action-plan/en/>
- 605 29. Fahrmeir L, Lang S. Bayesian inference for generalized additive mixed
606 models based on Markov random field priors. *J R Stat Soc Ser C Appl Stat*
607 2001; 50(2):201-20.
- 608 30. Held L, Natário I, Fenton SE, Rue H, Becker N. Towards joint disease
609 mapping. *Stat Methods Med Res* 2005; 14(1):61-82.
- 610 31. Goicoa T, Ugarte MD, Etxeberria J, Militino AF. Age-space-time CAR models
611 in Bayesian disease mapping. *Stat Med* 2016; 35(14):2391-405.
- 612 32. Clayton DG. Bayesian methods for mapping disease risk. *Geographical and*
613 *environmental epidemiology: methods for small-area studies*. 1992:205-220.
- 614 33. Richardson S, Thomson A, Best N, Elliott P. Interpreting posterior relative risk
615 estimates in disease-mapping studies. *Environ Health Perspect* 2004;
616 112(9):1016.
- 617 34. Ugarte MD, Goicoa T, Militino AF. Empirical Bayes and Fully Bayes
618 procedures to detect high-risk areas in disease mapping. *Comput Stat Data*
619 *An* 2009; 53(8):2938-49.
- 620 35. Hansell AL, Ghosh RE, Fecht D, Fortunato L. *The environment and health*
621 *atlas for England and Wales*. Oxford University Press, Oxford, England 2014.
- 622 36. Knorr-Held L, Best NG. A shared component model for detecting joint and
623 selective clustering of two diseases. *J R Stat Soc Ser A Stat Soc* 2001;
624 164(1):73-85.
- 625 37. Richardson S, Abellan JJ, Best N. Bayesian spatio-temporal analysis of joint
626 patterns of male and female lung cancer risks in Yorkshire (UK). *Stat*
627 *Methods Med Res* 2006; 15(4):385-407.
- 628 38. Mahaki B, Mehrabi Y, Kavousi A, Schmid VJ. A Spatio-Temporal Multivariate
629 Shared Component Model with an Application in Iran Cancer Data. *arXiv*
630 preprint arXiv:1707.06075. 2017 Jul 19.

- 1
2
3 631 39. Etxeberria J, Goicoa T, Ugarte MD. Joint modelling of brain cancer incidence
4 632 and mortality using Bayesian age-and gender-specific shared component
5 633 models. *Stoch Environ Res Risk Assess* 2018; 1-9.
- 6 634 40. Boulieri A, Liverani S, Hoogh K, Blangiardo M. A space–time multivariate
7 635 Bayesian model to analyse road traffic accidents by severity. *J R Stat Soc Ser*
8 636 *A Stat Soc* 2017; 180(1):119-39.
- 9 637 41. Abellan JJ, Richardson S, Best N. Use of space–time models to investigate
10 638 the stability of patterns of disease. *Environ Health Perspect*
11 639 2008;116(8):1111.
- 12 640 42. Duncan EW, White NM, Mengersen K. Bayesian spatiotemporal modelling for
13 641 identifying unusual and unstable trends in mammography utilisation. *BMJ*
14 642 *open* 2016; 6(5):e010253.
- 15 643 43. Li G, Best N, Hansell AL, Ahmed I, Richardson S. BaySTDetect: detecting
16 644 unusual temporal patterns in small area data via Bayesian model choice.
17 645 *Biostatistics* 2012; 13(4):695-710.
- 18 646 44. Boulieri A, Hansell A, Blangiardo M. Investigating trends in asthma and
19 647 COPD through multiple data sources: a small area study. *Spat*
20 648 *Spatiotemporal Epidemiol* 2016; 19:28-36.
- 21 649 45. Li G, Haining R, Richardson S, Best N. Space–time variability in burglary risk:
22 650 a Bayesian spatio-temporal modelling approach. *Spat Stat* 2014; 9:180-91.
- 23 651 46. Durban JW, Weller DW, Lang AR, Perryman WL. Estimating gray whale
24 652 abundance from shore-based counts using a multilevel Bayesian model. *J*
25 653 *Cetacean Res Manage* 2015; 15:61-8.
- 26 654 47. Boulieri A, Bennett J, Blangiardo M. Bayesian mixture modelling approach for
27 655 public health surveillance, *Biostatistics* 2018 (to appear).
- 28 656 48. Ito I, Kawaguchi Y, Kawasaki A, Hasegawa M, Ohashi J, Kawamoto M,
29 657 Fujimoto M, Takehara K, Sato S, Hara M, Tsuchiya N. Association of the
30 658 FAM167A–BLK region with systemic sclerosis. *Arthritis Rheumatol* 2010;
31 659 62(3):890-5.
- 32 660 49. Morin A, Laviolette M, Pastinen T, Boulet LP, Laprise C. Combining omics
33 661 data to identify genes associated with allergic rhinitis. *Clin Epigenetics* 2017;
34 662 9(1):3.
- 35 663 50. Benjamini Y, Hochberg Y. Controlling the false discovery rate: a practical and
36 664 powerful approach to multiple testing. *J R Stat Soc Series B Stat Methodol*
37 665 1995; 289-300.
- 38 666 51. Catelan D, Biggeri A. Multiple testing in disease mapping and descriptive
39 667 epidemiology. *Geospat Health* 2010; 4(2):219-29.
- 40 668 52. Storey JD. The positive false discovery rate: a Bayesian interpretation and the
41 669 q-value. *Ann Stat* 2003; 31(6):2013-35.
- 42 670 53. Newton MA, Noueiry A, Sarkar D, Ahlquist P. Detecting differential gene
43 671 expression with a semiparametric hierarchical mixture method. *Biostatistics*
44 672 2004; 5(2):155-76.
- 45 673 54. Muller P, Parmigiani G, Rice K. FDR and Bayesian multiple comparisons
46 674 rules. In *Proceedings Valencia*. 2006.
- 47 675 55. Scott JG, Berger JO. An exploration of aspects of Bayesian multiple testing. *J*
48 676 *Stat Plan Inference* 2006; 136(7):2144-62.
- 49 677 56. Whittemore AS. A Bayesian false discovery rate for multiple testing. *J Appl*
50 678 *Stat* 2007; 34(1):1-9.
- 51 679 57. Ventrucci M, Scott EM, Cocchi D. Multiple testing on standardized mortality
52 680 ratios: a Bayesian hierarchical model for FDR estimation. *Biostatistics* 2010;
53 681 12(1):51-67.
- 54 682 58. Gelman A, Hill J, Yajima M. Why we (usually) don't have to worry about
55 683 multiple comparisons. *J Res Educ Eff* 2012; 5(2):189-211.

1
2
3
4
5
6
7
8
9
10
11
12
13
14
15
16
17
18
19
20
21
22
23
24
25
26
27
28
29
30
31
32
33
34
35
36
37
38
39
40
41
42
43
44
45
46
47
48
49
50
51
52
53
54
55
56
57
58
59
60

- 684 59. Foreman KJ, Li G, Best N, Ezzati M. Small area forecasts of cause-specific
685 mortality: application of a Bayesian hierarchical model to US vital registration
686 data. *J R Stat Soc Ser C Appl Stat* 2017; 66(1):121-39.
- 687 60. Spiegelhalter DJ, Thomas A, Best NG, Gilks W, Lunn D. BUGS: Bayesian
688 inference using Gibbs sampling. Version 0.5,(version ii) [http://www.mrc-bsu.](http://www.mrc-bsu.cam.ac.uk/bugs)
689 [cam.ac.uk/bugs](http://www.mrc-bsu.cam.ac.uk/bugs). 1996; 19.
- 690 61. Carpenter B, Gelman A, Hoffman MD, Lee D, Goodrich B, Betancourt M,
691 Brubaker M, Guo J, Li P, Riddell A. Stan: A probabilistic programming
692 language. *J Statis Softw* 2017; 76(1).
- 693 62. de Valpine P, Turek D, Paciorek CJ, Anderson-Bergman C, Lang DT, Bodik
694 R. Programming with models: writing statistical algorithms for general model
695 structures with NIMBLE. *J Comput Graph Stat* 2017; Apr 3;26(2):403-13.
- 696 63. Rue H, Martino S, Chopin N. Approximate Bayesian inference for latent
697 Gaussian models by using integrated nested Laplace approximations. *J R*
698 *Stat Soc Series B Stat Methodol* 2009; 71(2):319-92.
- 699 64. Ugarte MD, Adin A, Goicoa T. One-dimensional, two-dimensional, and three
700 dimensional B-splines to specify space–time interactions in Bayesian disease
701 mapping: Model fitting and model identifiability. *Spat Stat* 2017; 22:451-68.
- 702 65. Anderson C, Lee D, Dean N. Identifying clusters in Bayesian disease
703 mapping. *Biostatistics* 2014; 15(3):457-69.
- 704 66. Adin A, Lee D, Goicoa T, Ugarte MD. A two-stage approach to estimate
705 spatial and spatio-temporal disease risks in the presence of local
706 discontinuities and clusters. *Stat Methods Med Res* 2018;
707 0962280218767975.
- 708 67. Ugarte MD, Goicoa T, Etxeberria J, Militino AF. Projections of cancer
709 mortality risks using spatio-temporal P-spline models. *Stat Methods Med Res*
710 2012; 21(5):545-60.
- 711 68. Corberán-Vallet A, Lawson AB. Prospective analysis of infectious disease
712 surveillance data using syndromic information. *Stat Methods Med Res* 2014;
713 Dec;23(6):572-90.
- 714 69. Diggle P, Rowlingson B, Su TL. Point process methodology for on-line spatio-
715 temporal disease surveillance. *Environmetrics* 2005; 16:423–434.
- 716 70. Diggle P, Moraga P, Rowlingson B, Taylor B. Spatial and Spatio-Temporal
717 Log-Gaussian Cox Processes: Extending the Geostatistical Paradigm. *Stat*
718 *Sci* 2013; 28(4):542-563.
- 719 71. Morrison KT, Shaddick G, Henderson SB, Buckeridge DL. A latent process
720 model for forecasting multiple time series in environmental public health
721 surveillance. *Stat Med* 2016; 35(18):3085-100.
- 722 72. Dai H, Lee BR, Hao J. Predicting asthma prevalence by linking social media
723 data and traditional surveys. *Ann Am Acad Pol Soc Sci* 2017; 669(1):75-92.
- 724 73. Wang Y, Pirani M, Hansell AL, Richardson S, Blangiardo M. Using ecological
725 propensity score to adjust for missing confounders in small area studies.
726 *Biostatistics* 2017; 1-16.
- 727 74. Gehlke CE, Biehl K. Certain effects of grouping upon the size of the
728 correlation coefficient in census tract material. *J Am Stat Assoc* 1934;
729 29(185A):169-70.
- 730 75. Openshaw S. The modifiable areal unit problem. Concepts and techniques in
731 modern geography. Geobooks 38, Norwich, England 1984;
- 732 76. Yiannakoulias N, Svenson LW, Schopflocher DP. An integrated framework for
733 the geographic surveillance of chronic disease. *Int J Health Geogr* 2009;
734 8(1):69.
- 735 77. Wakefield J, Lyons H. Spatial aggregation and the ecological fallacy. In
736 *Handbook of Spatial Statistics*. London, CRC Press, 2010: 541-58.

- 1
2
3 737 78. Jarup L. Health and environment information systems for exposure and
4 738 disease mapping, and risk assessment. Environ Health Perspect 2004;
5 739 112(9):995.
6 740 79. Moraga P. SpatialEpiApp: A Shiny web application for the analysis of spatial
7 741 and spatio-temporal disease data. Spat Spatiotemporal Epidemiol 2017;
8 742 23:47-57.
9
10
11
12
13
14
15
16
17
18
19
20
21
22
23
24
25
26
27
28
29
30
31
32
33
34
35
36
37
38
39
40
41
42
43
44
45
46
47
48
49
50
51
52
53
54
55
56
57
58
59
60

For Review Only

	FDR	FOR	Sensitivity	Specificity
DM1	0.785 (0.773, 0.800)	0.002 (0.000, 0.006)	0.979 (0.933, 1.000)	0.722 (0.695, 0.744)
DM2	0.191 (0.100, 0.267)	0.026 (0.020, 0.030)	0.660 (0.600, 0.733)	0.987 (0.981, 0.995)
STmix1	0.000 (0.000, 0.000)	0.017 (0.010, 0.024)	0.773 (0.683, 0.867)	1.000 (1.000, 1.000)
STmix2	0.220 (0.167, 0.300)	0.002 (0.000, 0.005)	0.969 (0.933, 1.000)	0.978 (0.969, 0.985)
FlexDetect	0.019 (0.015, 0.031)	0.005 (0.004, 0.006)	0.796 (0.763, 0.827)	1.000 (0.999, 1.000)

Table1: Results of the simulation study to compare the detection performance of disease mapping (DM), the mixture model on the spatio-temporal interaction (STmix1, STmix2) and the mixture model on the spatio-temporal rates (FlexDetect).

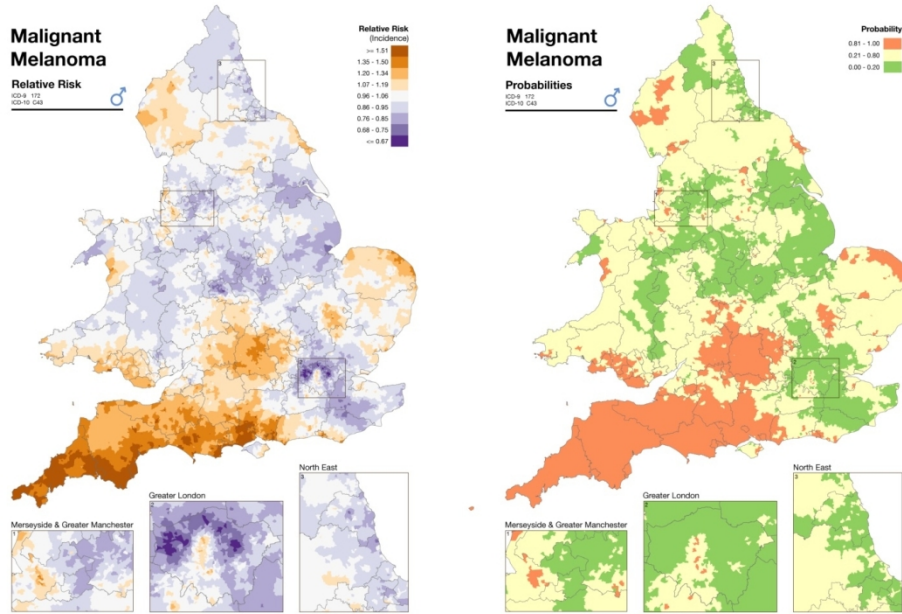


Figure 1: Area specific posterior mean relative risk of malignant melanoma (left) and posterior probability that an area is characterised by a relative risk above 1 (right). Source: Environment and Health Atlas [42].

548x386mm (72 x 72 DPI)

1
2
3
4
5
6
7
8
9
10
11
12
13
14
15
16
17
18
19
20
21
22
23
24
25
26
27
28
29
30
31
32
33
34
35
36
37
38
39
40
41
42
43
44
45
46
47
48
49
50
51
52
53
54
55
56
57
58
59
60

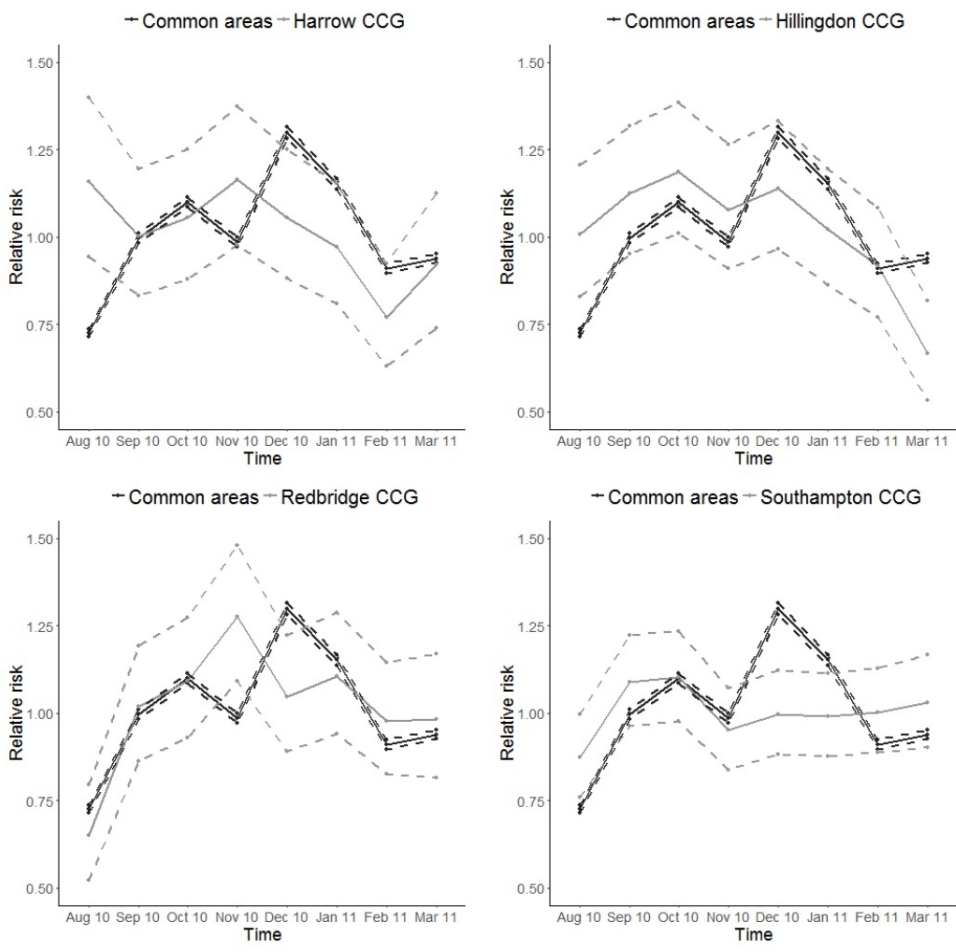


Figure 2: Relative risks and 95% credible intervals of hospital admissions for asthma and COPD for the national (common) temporal trend and for four areas classified as unusual.

377x371mm (72 x 72 DPI)